TELKOMNIKA, Vol.17, No.6, December 2019, pp.2842~2850
ISSN: 1693-6930, accredited First Grade by Kemenristekdikti, Decree No: 21/E/KPT/2018
DOI: 10.12928/TELKOMNIKA.v17i6.12838

Impact of Gouy-Chapman-Stern model on conventional ISFET sensitivity and stability

Ahmed M. Dinar*[1], AS Mohd Zain[2], F. Salehuddin[3], M.K. Abdulhameed[4], Mowafak K. Mohsen[5], Mothana L. Attiah[6]
[1,2,3,4,5]Faculty of Electronics and Computer Engineering, Universiti Teknikal Malaysia Melaka (UTeM), Malacca, Malaysia
[1]Computer Engineering, University of Technology, Baghdad, Iraq
*Corresponding author, e-mail: aealzubydi@gmail.com

Abstract

Utilizing Gouy-Chapman-Stern model can improve ISFET sensitivity and stability using Stern layer in direct contact with electrolyte in ISFET sensing window. However, this model remains a challenge in mathematical way, unless it's re-applied using accurate simulation approaches. Here, we developed an approach using a commercial Silvaco TCAD to re-apply Gouy-Chapman-Stern model as ISFET sensing membrane to investigate its impact on sensitivity and stability of conventional ISFET. Sio_2 material and high-k Ta_2O_5 material have been examined based on Gouy-Chapman and Gouy-Chapman-Stern models. Results shows that the ISFET sensitivity of SiO_2 sensing membrane is improved from ~38 mV/pH to ~51 mV/pH and the V_{TH} shift stability is also improved. Additionally, the results indicate that the sensitivity of Ta_2O_5 is 59.03 mV/pH that hit the Nearnst Limit 59.3 mV/pH and achieves good agreements with mathematical model and previous experimental results. In conclusion, this investigation introduces a real validation of previous mathematical models using commercial TCAD approach rather than expensive fabrication that paves the way for further analysis and optimization.

Keywords*: Gouy-Chapman-Stern, high-k, ISFET sensitivity, stability, stern layer*

1. Introduction

CMOS technology now provides an opportunity for chemical sensing platforms to leverage semiconductor technology that may offer advantages such as scalability, miniaturisation, fabrication, and integration with intelligent instrumentation. ISFET sensors are the most promising, and may satisfy all these opportunities. Due to its promising application in biological, biochemical and medical detection [1-5], ISFET has received much interest since it was first reported by Bergveld in 1972 [6]. Particularly, much effort has been made to investigate pH sensitive ISFETs with studies on device structures and pH-sensing membranes aimed at improving the sensitivity and stability of ISFETs [7, 8]. It is well known that the gate dielectric is in direct contact with the electrolyte solution, which determines the starting sensitivity of these devices. As the SiO_2 gate dielectric shows a low response sensitivity and poor stability, other inorganic materials such as Al_2O_3 [8, 9], Si_3N_4 [7, 10], Ta_2O_5 [9, 11], HfO_2 [12-15] and ZrO_2 [12-14] with their enhanced stability and sensitivity have also been investigated.

Until now, different models and adaptations of models have been used to model the pH-change sensitivity in ISFETs, the development of surface potential in the area, and in the further course of a Helmholtz double layer (DL). Louis Georges Gouy in 1910, and David Leonard Chapman in 1913, together noticed that capacitance was not a constant, but depended on the applied potential and the ionic concentration. The Gouy-Chapman model made an important contribution by proposing a diffuse model of the DL. In this model, "the charge distribution of ions as a function of distance from the metal surface allows Maxwell-Boltzmann statistics to be applied". Thus, the electric potential decreases exponentially at distances further away from the surface of the fluid bulk. However, the Gouy-Chapman model fails for highly charged DLs. In 1924, Otto Stern suggested combining the Helmholtz model with the Gouy-Chapman model: In Stern's model, some ions adhere to the electrode as suggested by Helmholtz, giving an internal Stern layer, while some form a Gouy-Chapman diffuse layer.

Received April 4, 2019; Revised June 1, 2019; Accepted July 2, 2019

Figure 1 demonstrates schematic representations of electrical double layer structures describing (a) the Helmholtz model, (b) the Gouy-Chapman model and (c) the Gouy-Chapman-Stern model.

This paper extends the previous investigations [16] that aimed at developing a different Models for simulation of ISFET operations. Particularly, in this work we examine more closely the links between IC design simulation and previous mathematical models have not be clearly linked and for more accurate analysis for further optimization.

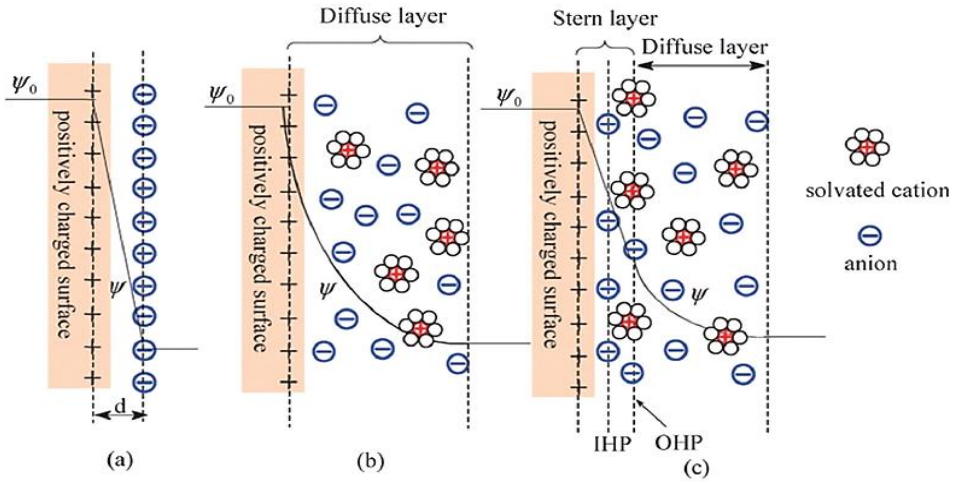

Figure 1. ISFET DL's models [15]

2. Material and Methods

2.1. Mathematical Model

In the original structure of an ISFET, the gate oxide is in direct contact with the electrolyte solution as shown in Figure 2 (a), acting as a sensing dielectric. The Stern layer is a modified version of the ISFET in which the sensing layer is separated from the gate oxide by using an extended conductive layer Figure 2 (b) after the gate oxide is covered by the electrolyte solution, creating a more robust structure for extended efficacy in the solutions. Through the effective coupling capacitance between the sensor surface and Floating Gate (FG), the surface potential (ψ_o) modulates the potential of the FG, and therefore there will be a corresponding shift in the threshold voltage (VT) of the sensor [17-21]. Therefore, from the Site-binding model, the charge density can be expressed by [19, 20, 22]:

$$\sigma_0 = qN_{sil}\left(\frac{aH_s^{+2} - K_aK_b}{K_aK_b + K_baH_s^{+} + aH_s^{+2}}\right) \quad (1)$$

where; aH_s^+ is the H^+ activity calculated by ($aH_s^+ = 10^{-pHs}$); q is the elementary charge; N_{sil} is the density of the available sites and K_a; K_b represents the intrinsic dissociation constants, and the N_{sil}, K_a and K_b, are oxide layer dependent.

Based on "charge density", the charge on the electrolyte side of a double layer (σDL) is the same value, but is a negative charge. Therefore, this charge can be calculated from the integral double layer capacitance (Ci) and the surface potential [23, 24]:

$$\sigma DL = -C_i\,\psi_\circ = -\sigma_\circ \quad (2)$$

Therefore, by solving (1) and (2), we can demonstrate the relation between aH_s^+ and ψ_o parameters. According to the Boltzmann distribution model for the H+ ions [9, 24], the pH value at the sensor surface is [9]:

$$pH_S = pH_B + \frac{q\,\psi_0}{2.3kT} \quad (3)$$

T and k represent the absolute temperature and Boltzmann constant, respectively. The subscript S and B denote the pH at the sensor surface and in the bulk solution, respectively, and ψo is the potential drop across the diffusion layer. In (3), the intrinsic buffer capacity (βint) is defined as the ability to collect a charge at the sensor surface (σ0) due to the change in surface pH (pHs) [9]:

$$\beta_{int} = \frac{\Delta\sigma_0}{-q\,\Delta pH_S} \tag{4}$$

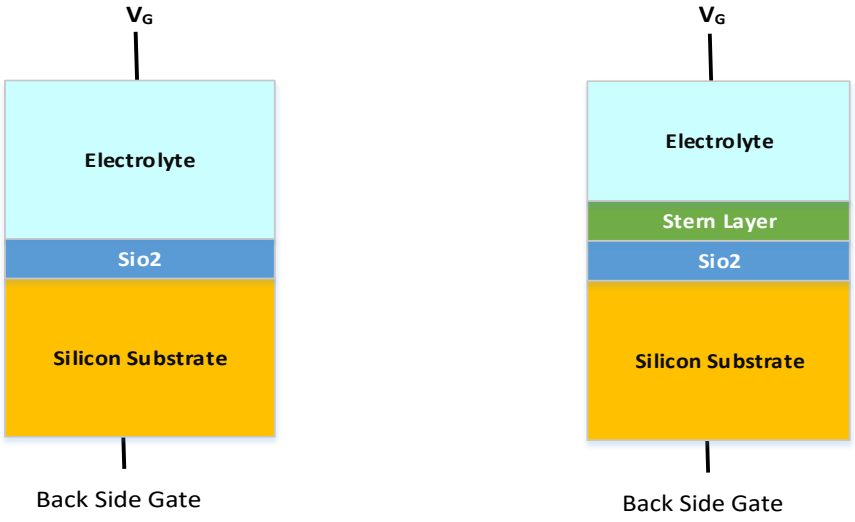

Figure 2. ISFET structure based on (a) chapman model (b) Gouy-Chapman-Stern model

The diffusion capacity (Cdiff) is the ability to store the opposing charge in the solution near the surface, due to the change in surface potential [9]:

$$C_{diff} = \frac{\Delta\sigma_0}{\Delta\psi_0} \tag{5}$$

therefore, we can write:

$$\frac{\Delta\psi_0}{\Delta pH_S} = -q\frac{\beta_{int}}{C_{diff}} \tag{6}$$

Differentiating (3) with respect to the bulk pH, and using (6), the surface potential sensitivity to the pH_B can be derived as [9]

$$\frac{\Delta\psi_0}{\Delta pH_B} = -2.3\frac{kT}{q}\left(\frac{1}{1+\alpha}\right) \tag{7}$$

with

$$\alpha = \frac{2.3\,k\,T\,C_{diff}}{q^2\,\beta_{int}} \tag{8}$$

here, α is a positive sensitivity (dimensionless parameter). Therefore, the sensitivity of the potential at the sensor surface and the corresponding change of the sensor threshold voltage to the bulk pH are limited to 59.3 mV/pH (Nernst limit). In the Stern model, the relationship between the diffusion layer potential ψ_o (previous calculations) and the Stern potential ψ_s can be expressed by:

$$(\psi o - \psi s) = \frac{(8kT\varepsilon\varepsilon_{\circ}n^{o})^{\frac{1}{2}}\ sinh\left(\frac{zq\psi s}{2kT}\right)}{C_S} \quad (9)$$

where $\varepsilon\varepsilon_{\circ}$ is the permittivity of free space and its relative permittivity, respectively; n^o is the number concentration of each ion in the bulk, z is the magnitude of the charge on the ions and C_S represents the integral capacitance of the Stern layer.

2.2. TCAD Simulation

Commercial TCAD allows users to introduce bias-dependent surface charges in the form of interface donor or acceptor traps. The challenge is simulating the updated surface charge density equation described by in the electrolyte pH change model [19]. To introduce this equation to the simulator, interface trap statements are utilized to mimic the surface charge accurately, as follows [21]:

INTTRAP <type> E. LEVEL= <r> DENSITY= <r> <capture parameters>

"INTTRAP" activates interface defect traps at discrete energy levels within the bandgap of the semiconductor and sets their parameter values. Device physics has established the existence of three different mechanisms, which add to the space charge term in Poisson's equation in addition to the ionized donor and acceptor impurities" [21]. Interface traps will add space charge directly into the right-hand side of Poisson's equation. To calculate the trapped charge in Poisson's equation, the total charge value is defined by the following:

$$\sigma_0 = q(N_{tD}^{+} - N_{tA}^{-}) \quad (10)$$

where N_{tD}^{+} and N_{tA}^{-} are the densities of ionized donor-like and acceptor-like traps, respectively. DENSITY and its probability of ionization are represented as *FtA* and *FtD*, respectively. For donor-like and acceptor-like traps, the ionized densities are calculated by the following equations:

$$N_{tD}^{+} = \text{DENSITY} \times F_{tD} \quad (11)$$

$$N_{tA}^{-} = \text{DENSITY} \times F_{tA} \quad (12)$$

where *FtA* and *FtD* are given by the following equations:

$$F_{tA} = \frac{V_n\ SIGN\ n + e_{pA}}{V_n\ SIGN\ n + V_p\ SIGP\ p + e_{nA} + e_{pA}} \quad (13)$$

$$F_{tD} = \frac{V_p\ SIGP\ p + e_{nD}}{V_n\ SIGN\ n + V_p\ SIGP\ p + e_{nD} + e_{pD}} \quad (14)$$

where *SIGN* is the carrier capture cross sections for electrons and *SIGP* holes. The thermal velocities for electrons and holes are V_n and V_p , respectively. For donor-like traps, the electron and hole emission rates, e_{nD} and e_{pD}, are defined by the following [21]:

$$e_{nD} = \frac{1}{DEGEN.FAC}\ V_n\ SIGN\ n_i\ e^{E_t - E_i / kT} \quad (15)$$

$$e_{pD} = DEGEN.FAC\ V_p\ SIGP\ n_i\ e^{E_i - E_t / kT} \quad (16)$$

where *Et and Ei are* the trap energy level and the intrinsic Fermi level position, respectively. DEGEN.FAC is the degeneracy factor of the trap center. For acceptor traps, the electron and hole emission rates, e_{nA} and e_{pA} , are defined by the following [21]:

$$e_{nA} = DEGEN.FAC\ V_n\ SIGN\ n_i\ e^{E_t - E_i / kT} \quad (17)$$

$$e_{pA} = \frac{1}{DEGEN.FAC} V_p \, SIGP \, n_i \, e^{E_i - E_t / kT} \quad (18)$$

For example, the acceptor interface trap statement and its parameters are as following:

INTTRAP ACCEPTOR E.LEVEL: DENSITY: INTMATERIAL: ***DEGEN.FAC*** *EoN: EoP:*

considering all equations mentioned above, we can rewrite the sit-binding model (1) based on TCAD model. We first assume that acceptor and donor traps exchange carriers only with the conduction and valence band of the semiconductor representing the electrolyte, respectively. Hence, we can rewrite (7) in terms of TCAD model as follows:

$$\sigma_{(TCAD)} = q \times DENSITY \left(\frac{V_P \, SIGP \, P - V_n SIGN \, n}{v_P \, SIGP \, P + V_n SIGN \, n + K_b n_i^2} \right) \quad (19)$$

for more details about TCAD simulation and modelling, the previous work was well described all modelling methodologies [25].

3. Result and Discussion

Models and simulation results have been shown in this section. In modeling part, Figure 3 examine the difference between Gouy-Chapman and Gouy-Chapman-Stern models using (8). The sensitivity parameter (α) (Dimensionless parameter) have been shown the sensitivity of surface potential changing based on range of pH bulk [21]. The value of a varies between 0 and 1 depending on the intrinsic buffer capacity and the differential capacitance [8]. Her we converted the values as proportions values from 0 to 59.3 that is the value of top Nearnst level. For a sensitivity close to the theoretical maximum, α approaches 59.3, the intrinsic buffer capacity should be high, and the differential capacitance should be small, as can be concluded from (8). A sensitivity close to zero can theoretically be derived when the intrinsic buffer capacity approaches zero. This shows that the Gouy-Chapman model remain challenge the Roll-off problem that already compensated by Gouy-Chapman-Stern models as we shown in Figure 3.

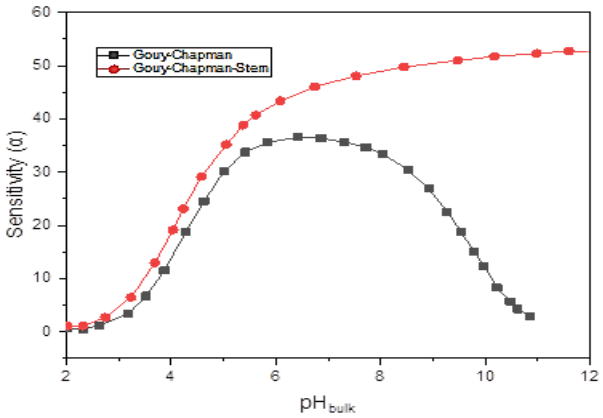

Figure 3. Theoretical sensitivity parameter

The theoretical surface potential shift based on range of pH bulk from pH2-pH12 were observed in Figure 4. The (7) and (9) are the expression for the sensitivity of the electrostatic potential to changes in the bulk pH [9]. As we shown the Sio_2 sensing membrane as Stern layer (9) achieve good agreement with experimental result in respect of sensitivity and stability. Nevertheless, A Sio_2 Gouy-Chapman model still have lack of curve stability as well as low sensitivity. On the other hand, Ta_2O_5 sensing membrane is behaved well in term of sensitivity

and stability comparing with normal silicon dioxide Which is known because high dielectric constant of high-k material. However, from mathematical models is very clear that using of Gouy-Chapman-Stern model enhance the ISFET sensitivity as well as achieve stable shift in surface potential through pH bulk change. On the other side, TCAD Simulaation results process is contribute same as modeling results. Table 1 and Table 2 are the TCAD simulation parameters.

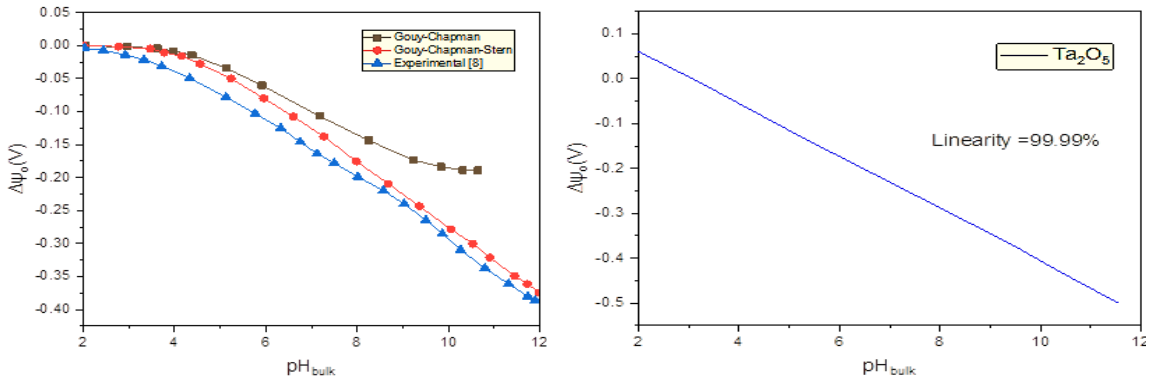

Figure 4. Theoretical surface potential shift (left) SiO_2 (right) Ta_2O_5

Table 1. TCAD Parameters of ISFET

Parameter	Value	Unit	Parameter	Value	Unit
t_{Stern}		-	Channel length	200	nm
T	300	K	S/D doping	10^{17}	cm^{-3}
k	1.380649×10−23	J/K	S/D length	50	nm
$t_{electrolyte}$	1000	Nm	Electrolyte concentration	10^{-3}	Mol/L
t_{ox}	3	Nm	Oxide permittivity	3.9	-
Electrolyte permittivity	80	-	V_{DS}	50	mV

Table 2. Materials Parameters used in TCAD Simulation

Material	Dilectric Constant	Density	K_a	K_b
Sio_2	3.9	$5 . 10^{14}$ (1/cm^2)	10^{-6}	10^{2}
Ta_2O5	22	$10 . 10^{14}$ (1/cm^2)	10^{-4}	10^{-2}

Figure 5 introduce the shifting in threshold voltage (V_{TH}) in range of pH bulk fron 2→12. indeed Shifting in threshold voltage sensitivity is the negetave values of shifting in surface potential based on the following expersion [24]:

$$\Delta V_{TH}=-\Delta\psi$$

However, the ISFET senssitivity and stability of conventional isfet for Sio_2 and Ta_2O_5 as a sensing membrane contribute very well comparing with ISFET whithout Stern layer as shown in Figure 5. As shown the linirity of Stern-ISFET is higher than ISFET whithout Stern as well as senstivity that consistent with behaviour of Figure 4. For more analysis, the average sensvity of conventinal Stern-ISFET for Ta2O5 sensing membarane is compared with the theoratical snestivity based on Nearnst equation observed in Figure 6. As shown the Ta_2O_5 is hit the Nearnst limit and the stability also contributed in acceptible way. The importantant aim is the linked between mathmatical model or physical interpretations and ISFET transfer charactrstics is introduced in Figure 7. In this Figure the real charactrization of pH bulk change with surface potential shifiting were demostrated. As shown, the drain current is slitly change with pH range from 1→14. Consequence, the main objective of this work is achived by linking the models whith real charactrization is clearly demostrated.

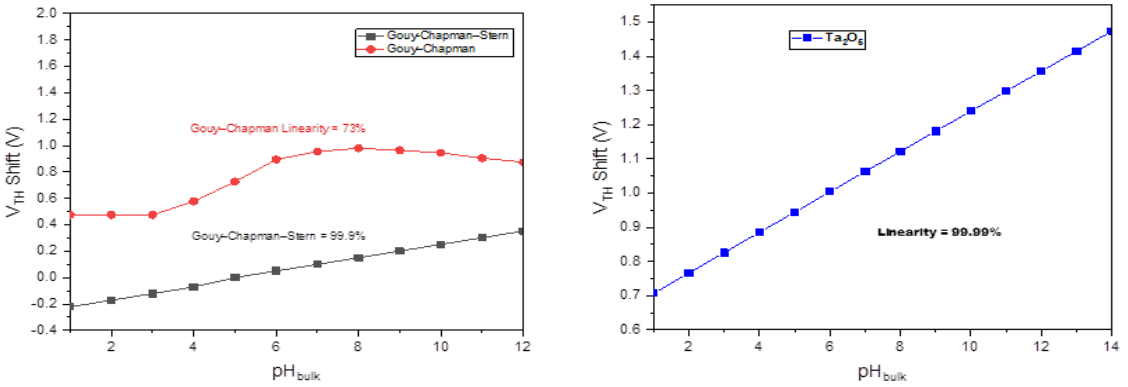

Figure 5. TCAD simulation threshold voltage shift (left) SiO_2 (right) Ta_2O_5

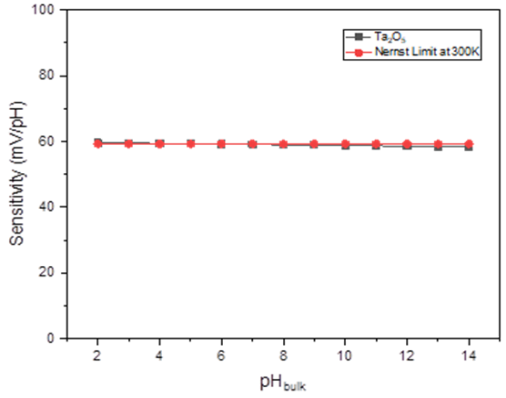

Figure 6. Average sensitivity of Ta_2O_5 sensing membarane

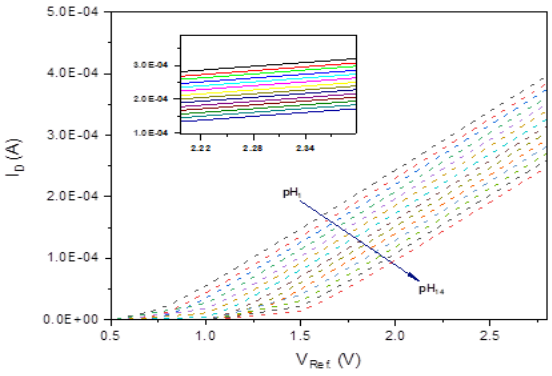

Figure 7. Conventinal ISFET drain current vs. refrence voltage of Ta_2O_5 sensing membarane

For more validation, Figure 8 introduce comparitive study for average sensitivity between mathmatical model, TCAD simulation, Nernst Limit as a refrence and other real experemnts. The comparsims show exelent agreement between Model and TCAD simulation for two material in Stern-ISFET. Despite of not good agreement with experemental value for Sio_2 because of lowermost of silicon deoxide, but our work achive exelent agreement with real experemental result in Ta_2O_5 sensing membarane as shown in Figure 8.

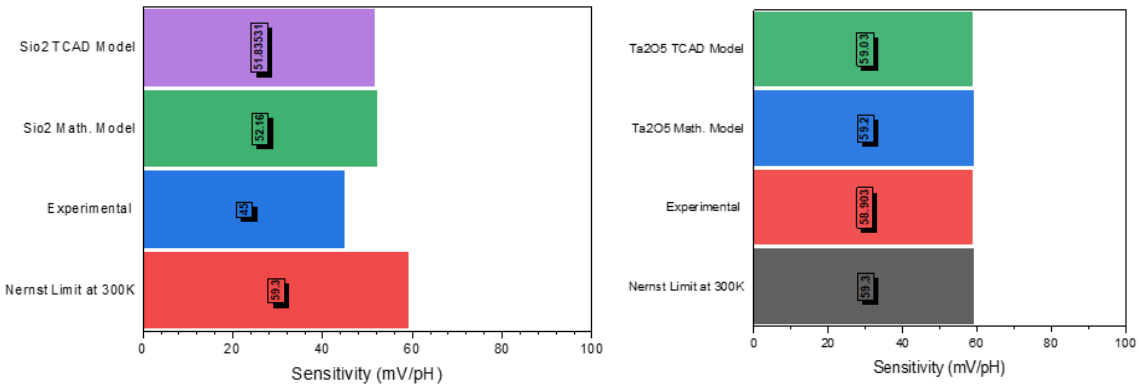

(Sio2) (Ta2O5)

Figure 8. Conventional ISFET comparison between model, simulation, nernst limit and experimental

4. Discussion

In contrast to the wide existence and importance of mathematical models for developing conventional ISFET sensitivity and ISFET concept as general, the link between these models and electrical characteristics simulation (i.e. TCAD) rather than expensive fabrication remain challenge. In this study, we adapted previous mathematical models and re-applied these models using commercial TCAD. We emphasise these models results and achieve good agreement with models as well as real experimental results for more validation. The above results show that utilizing of Gouy-Chapman-Stern model will increase the conventional ISFET sensitivity and stability of normal silicon dioxide as well as high-k materials comparing with Gouy-Chapman model. For ISFET sensitivity with Sio2 sensing membrane is raised from ~38 mV/pH to ~51 mV/pH, And, Ta_2O_5 is hit the Nernst Limit (59.3 mV/pH) by value of 59.03 mV/pH. Furthermore, using of Stern Layer is compensate the Roll-off problem in normal model by enhancement of threshold voltage shifts linearity to reach 99.9% and 99.999% in Sio_2 and Ta_2O_5 sensing membranes, respectively.

Further studies should investigate the performance analysis of commonly used high-k materials using same approach. Although the simulation approach still considered not real fabrication and measurements, this study opens new directions for further analysis and optimization prior the real and cost-effective fabrication way.

5. Conclusion

In this work we examine more closely the links between IC design simulation and previous mathematical models have not be clearly linked and for more accurate analysis. we adapted previous mathematical models and re-applied these models using commercial TCAD. ISFET sensitivity with Sio_2 sensing membrane is raised from ~38 mV/pH to ~51 mV/pH, And, Ta_2O_5 is hit the Nernst Limit (59.3 mV/pH) by value of 59.03 mV/pH. Furthermore, using of Stern Layer is compensate the Roll-off problem in normal model by enhancement of threshold voltage shifts linearity to reach 99.9% and 99.999% in Sio_2 and Ta_2O_5 sensing membranes, respectively. We anticipate this study opens new directions for further analysis and optimization prior the real and cost-effective fabrication way.

Acknowledgment

The authors gratefully acknowledge the UTeM Zamalah Scheme, Universiti Teknikal Malaysia Melaka (UTeM), and the supports from the Centre for Research and Innovation Management (CRIM), Centre of Excellence, Universiti Teknikal Malaysia Melaka (UTeM).

References

[1] A Bratov, N Abramova, C Domínguez. Investigation of chloride sensitive ISFETs with different membrane compositions suitable for medical applications. *Anal. Chim. Acta*. 2004; 514(1): 99-106.
[2] AM Dinar, ASM Zain, F Salehuddin, "CMOS ISFET device for DNA Sequencing : Device Compensation, Application Requirements and Recommendations. *Int. J. Appl. Eng. Res.* 2017; 12(21): 11015–11028.
[3] CS Lee, S Kyu Kim, M Kim. Ion-sensitive field-effect transistor for biological sensing. *Sensors*. 2009; 9(9): 7111-7131.
[4] T Sakurai, Y Husimi. Real-Time Monitoring of DNA Polymerase Reactions by a Micro ISFET pH Sensor. *Anal. Chem.* 1992; 64(17): 1996-1997.
[5] AM Dinar, ASM Zain, F Salehuddin. Utilizing Of Cmos Isfet Sensors In Dna Applications Detection : A Systematic Review. *Jour Adv Res. Dyn. Control Syst.* 2018; 10(04): 569-583.
[6] P Bergveld. Development, operation, and application of the ion-sensitive field-effect transistor as a tool for electrophysiology. *IEEE Trans. Biomed. Eng.* 1972; 19(5): 342-351.
[7] MN Niu, XF Ding, QY Tong. Effect of two types of surface sites on the characteristics of Si3N4-gate pH-ISFETs. *Sensors Actuators B Chem.* 1996; 37(1-2): 13-17.
[8] S Chen, JG Bomer, ET Carlen, A Van Den Berg. Al2O3/silicon nanoISFET with near ideal nernstian response. *Nano Lett.* 2011; 11(6): 2334-2341.
[9] REG Van Hal, JCT Eijkel, P Bergveld. A general model to describe the electrostatic potential at electrolyte oxide interfaces. *Adv. Colloid Interface Sci.* 1996; 69(1-3): 31-62.
[10] DL Harame, LJ Bousse, JD Shott, JD Meindl. Ion-Sensing Devices with Silicon Nitride and Borosilicate Grlass Insulators. *IEEE Trans. Electron Devices*. 1987; 34(8): 1700-1707.

[11] DH Kwon, BW Cho, CS Kim, BK Sohn. Effects of heat treatment on Ta2O5 sensing membrane for low drift and high sensitivity pH-ISFET. *Sensors Actuators B Chem.* 1996; 34(1-3): 441-445.
[12] T Akiyama, Y Ujihira, Y Okabe, T Sugano, E Niki. Ion-Sensitive Field-Effect Transistors with Inorganic Gate Oxide for pH Sensing. *IEEE Trans. Electron Devices*. 1982; 29(12): 1936-1941.
[13] HR Thakur, G Keshwani, JC Dutta, C. Engineering. Sensitivity of Carbon Nanotube Based Junctionless Ion Sensitive Field Effect Transistor (CNTJLISFET) for HfO2 and ZrO2 gate dielectrics: *Experimental and Theoretical Investigation*. 2017: 137-142.
[14] V Jankovic, JP Chang. HfO2 and ZrO2-Based Microchemical Ion Sensitive Field Effect Transistor (ISFET) Sensors: Simulation & Experiment. *J. Electrochem. Soc.* 2011; 158(10): P115-P117.
[15] A Tarasov *et al.*. Understanding the electrolyte background for biochemical sensing with ion-sensitive field-effect transistors. *ACS Nano*. 2012; 6(10): 9291-9298.
[16] AM Dinar, AS Mohd Zain, F Salehuddin. Comprehensive identification of sensitive and stable isfet sensing layer high-k gate based on isfet/electrolyte models. *Int. J. Electr. Comput. Eng.* 2019; 9(2): 926-933.
[17] B Chen, A Parashar, S Pandey. Folded floating-gate CMOS biosensor for the detection of charged biochemical molecules. *IEEE Sens. J.* 2011. 11(11): 2906-2910.
[18] LL Chi, JC Chou, WY Chung, TP Sun, SK Hsiung. Study on extended gate field effect transistor with tin oxide sensing membrane. *Mater. Chem. Phys.* 2000; 63(1): 19-23.
[19] W Healy, DE Yates, S Levine. Site-binding Model of the Electrical Double Layer at the Oxide/Water Interface. *Trans. Farad. Soc. I*. 1974; 70: 1807-1818.
[20] E Mohammadi, N Manavizadeh. *Performance and sensitivity analysis of Dual-gated ion sensitive*. FET. 2017 25th Iran. Conf. Electr. Eng. ICEE 2017, no. lCEE20 17. 2017: 440-444.
[21] DS. Software. ATLAS User' s Manual. 2016; 408: 567-1000.
[22] KB Parizi, X Xu, A Pal, X Hu, HS Philip Wong. ISFET pH Sensitivity: Counter-Ions Play a Key Role. *Sci. Rep.* 2017; 7(3): 1-10.
[23] TM Pan, S Mondal. Structural Properties and Sensing Characteristics of Sensing Materials. Comprehensive Materials Processing. 2014; 13: 179-203.
[24] HJ Jang, WJ Cho. Fabrication of high-performance fully depleted silicon-on-insulator based dual-gate ion-sensitive field-effect transistor beyond the Nernstian limit. *Appl. Phys. Lett.* 2012; 100: 7.
[25] AM Dinar, A Mohd Zain, F Salehuddin, ML Attiah, MK Abdulhameed, MK Mohsen. *Modeling and simulation of electrolyte pH change in conventional ISFET using commercial Silvaco TCAD*. in IOP Conference Series: Materials Science and Engineering. 2019; 518: 042020.